

Volume Title

ASP Conference Series, Vol. **Volume Number**

Author

© **Copyright Year** Astronomical Society of the Pacific

Dissecting Kinematics and Stellar Populations of Counter-Rotating Galaxies with 2-Dimensional Spectroscopy

L. Coccato,^{1,2} L. Morelli,^{3,4} A. Pizzella,³ E. M. Corsini,^{3,4} E. Dalla Bontà,^{3,4}
and L. M. Buson⁴

¹*European Southern Observatory, Garching bei München, Germany*

²*Institute of Cosmology and Gravitation, University of Portsmouth,
Portsmouth, UK*

³*Dipartimento di Fisica ed Astronomia ‘Galileo Galilei’, Università di Padova,
Padova, Italy*

⁴*INAF-Osservatorio Astronomico di Padova, Padova, Italy*

Abstract. We present a spectral decomposition technique and its applications to a sample of galaxies hosting large-scale counter-rotating stellar disks. Our spectral decomposition technique allows to separate and measure the kinematics and the properties of the stellar populations of both the two counter-rotating disks in the observed galaxies at the same time. Our results provide new insights on the epoch and mechanism of formation of these galaxies.

1. Introduction

Some galaxies, despite of their simple morphologies, can reveal to be very complex systems from a kinematic point of view. Clear examples are objects with stars and/or gas in orthogonal rotation with respect the rest of the galaxy (e.g., Corsini et al. 2003; Coccato et al. 2004; Corsini et al. 2012), or with a warped inner structure (e.g., Coccato et al. 2007). Among these galaxies with multi-spin components, *counter-rotating galaxies* are those that host two components that rotate in opposite directions from each other. These peculiar objects have been observed from in all morphological types. They are classed by the nature (stars vs. stars, stars vs. gas, gas vs. gas) and size (counter-rotating cores, rings, and disks) of the counter-rotating components (see Bertola & Corsini 1999, for a review). The subject of this work is the peculiar case of galaxies hosting two counter-rotating stellar disks of comparable size. The prototype of this class of objects is the famous E7/S0 galaxy NGC 4550, whose counter-rotating nature was first discovered by Rubin et al. (1992).

The study of the kinematics and the stellar population of the two counter-rotating components are the key to understand the formation mechanisms of these objects. This task is complicated by the fact that the two components are co-spatial, and therefore we observe their combined contribution at each position on the sky. Thus, it is necessary to separate their contribution to the total observed galaxy spectrum and measure the properties and kinematics of their stellar populations separately. To this aim we devel-

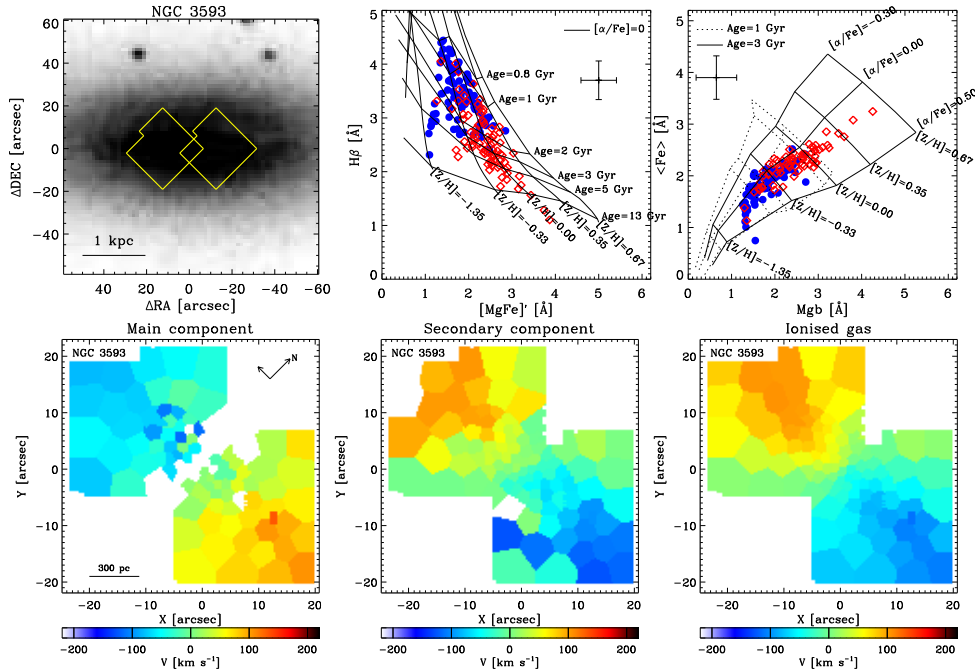


Figure 1. Results of the spectroscopic decomposition in NGC 3593. Top panels: Observed field of view, absorption line indices, and prediction from stellar population models (Thomas et al. 2011); red and blue symbols refer to the main and secondary stellar components, respectively. Bottom panels: 2-dimensional velocity fields of the main and secondary stellar components, and of the ionized gas component.

oped a spectroscopic decomposition technique and successfully applied to three spiral galaxies with counter-rotating stellar disks (Cocato et al. 2011, 2013a,b).

2. Analysis: Spectroscopic Decomposition

We observed with the Visible Multi Object Spectrograph (VIMOS) integral-field unit at the Very Large Telescope (VLT) three spiral galaxies, which are known to host counter-rotating stellar disks: NGC 3593 (Bertola et al. 1996), NGC 4550 (Rubin et al. 1992), and NGC 5197 (Vergani et al. 2007). Our spectroscopic decomposition technique exploits the differences in kinematics and stellar populations of the two components to separate their contribution from the combined observed spectrum. At each position on the galaxy, the code builds two synthetic templates (one for each stellar component) as linear combination of spectra from an input stellar library, and convolves them with two Gaussian line-of-sight velocity distributions with different kinematics. Gaussian functions are also added to the convolved synthetic templates to account for ionized-gas emission lines ($\text{H}\gamma$, $\text{H}\beta$, $[\text{O III}]$, and $[\text{N I}]$). The spectroscopic decomposition code returns the spectra of two best-fit stellar templates (that represent the two stellar disks) and ionized-gas emissions, along with the best-fitting parameters of luminosity of each component, velocity, and velocity dispersion. The line strength of the Lick indices of

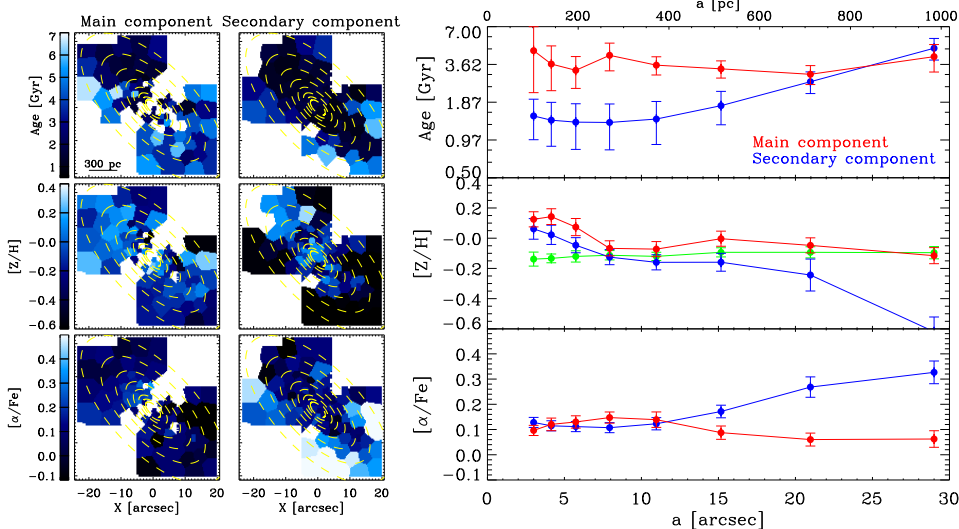


Figure 2. Stellar population parameters in NGC 3593. Left panels: Maps of the age, metallicity, and α -enhancement of the two stellar counter-rotating components, as derived by fitting the Thomas et al. (2011) models to the measured Lick indices. Right panels: Radial profiles of the total luminosity-weighted age, metallicity, and α -enhancement within concentric ellipses.

the two counter-rotating components are measured on the two best-fit stellar templates. The line strength of the absorption line indices are then used to infer the age, metallicity, abundance ratios, stellar mass-to-light ratio, and the stellar mass of the two stellar components.

3. Results of the Spectroscopic Decomposition

We successfully separated the contribution of the ionized gas and the two stellar components from the observed spectrum, and confirm the presence of two counter-rotating stellar disks in NGC 3593. More details on this galaxy and other galaxies in our sample are in Coccato et al. (2011, 2013a).

Fig. 1 shows the observed field of view, the 2-dimensional velocity fields of the stellar and ionized gas components, and the line strength of the absorption line indices ($H\beta$, $Mg\ b$, $[MgFe]$, and $\langle Fe \rangle$). Fig. 2 shows the 2-dimensional maps of the age, metallicity and α -enhancement, and their radial profiles. Fig. 3 shows the radial profiles of the stellar mass-to-light ratio and the mass of the two components.

The secondary disk is on average less luminous and less massive than the main stellar disk, and it rotates along the same direction as the ionized gas component. The two counter-rotating stellar components have different stellar populations. The secondary stellar disk is younger, more metal poor, and more α -enhanced than the main galaxy stellar disk. The age difference between the two components is higher within 500 pc: the main component is (3.7 ± 0.6) Gyr old, whereas the secondary component is (1.4 ± 0.2) Gyr old. From the difference in age of the two components, we are able to date the formation of the counter-rotating stellar disk to ~ 2 Gyr ago, i.e. ~ 1.6

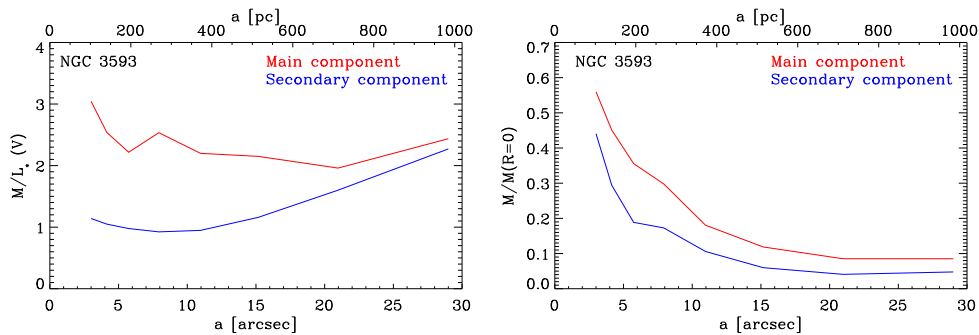


Figure 3. Left panel: Radial profiles of the mass-to-light ratio in the V band for NGC 3593. Right panel: Mass surface density profiles relative to the central value for NGC 3593.

Gyr after the formation of the main galaxy disk. Both components have high metallicity in the central 150 pc followed by a declining profile. The main component is on average more metal rich ($[Z/H]_1 = -0.04 \pm 0.03$) than the secondary component ($[Z/H]_2 = -0.15 \pm 0.07$).

4. Conclusions

Our results rule out internal processes, such as bar dissolution, since they would lead to the formation of two counter-rotating disks with the same properties.

External acquisition of gas followed by star formation, or mergers of two galaxies with similar mass are both viable mechanisms. The accretion scenario predicts that the secondary component is the younger, and that the two components have different metallicity, as they are formed from different gas clouds. In the second scenario, the properties of the two stellar component depend on the properties of the merging systems and star formation episodes triggered by the merger.

A larger sample is therefore required to statistically determine which mechanism is the most efficient to build counter-rotating stellar disks.

References

- Bertola, F., Cinzano, P., Corsini, E. M., et al. 1996, *ApJ*, 458, L67
 Bertola, F., & Corsini, E. M. 1999, in *IAU Symp. 186, Galaxy Interactions at Low and High Redshift*, ed. J. E. Barnes, & D. B. Sanders (Dordrecht: Kluwer), 149
 Cocato, L., Corsini, E. M., Pizzella, A., et al. 2004, *A&A*, 416, 507
 — 2007, *A&A*, 416, 507
 Cocato, L., Morelli, L., Corsini, E. M., et al. 2011, *MNRAS*, 412, L113
 Cocato, L., Morelli, L., Pizzella, A., et al. 2013a, *The Messenger*, 151, 33
 — 2013b, *A&A*, 549, A3
 Corsini, E. M., Méndez-Abreu, J., Pastorello, et al. 2012, *MNRAS*, 423, L79
 Corsini, E. M., Pizzella, A., Cocato, L., et al. 2003, *A&A*, 408, 873
 Rubin, V. C., Graham, J. A., & Kenney, J. D. P. 1992, *ApJ*, 394, L9
 Thomas, D., Maraston, C., & Johansson, J. 2011, *MNRAS*, 412, 2183
 Vergani, D., Pizzella, A., Corsini, et al. 2007, *A&A*, 463, 883